Profiling locomotor recovery: comprehensive quantification of impairments after CNS damage in rodents

Björn Zörner[1,3], Linard Filli[1,3], Michelle L Starkey[1], Roman Gonzenbach[1], Hansjörg Kasper[1], Martina Röthlisberger[1], Marc Bolliger[2] & Martin E Schwab[1]

Rodents are frequently used to model damage and diseases of the central nervous system (CNS) that lead to functional deficits. Impaired locomotor function is currently evaluated by using scoring systems or biomechanical measures. These methods often suffer from limitations such as subjectivity, nonlinearity and low sensitivity, or focus on a few very restricted aspects of movement. Thus, full quantitative profiles of motor deficits after CNS damage are lacking. Here we report the detailed characterization of locomotor impairments after applying common forms of CNS damage in rodents. We obtained many objective and quantitative readouts from rats with either spinal cord injuries or strokes and from transgenic mice (*Epha4*$^{-/-}$) during skilled walking, overground walking, wading and swimming, resulting in model-specific locomotor profiles. Our testing and analysis method enables comprehensive assessment of locomotor function in rodents and has broad application in various fields of life science research.

A common consequence of damage to the CNS caused by trauma, ischemia, or neurodegenerative or inflammatory diseases is impairment of motor functions. In the corresponding animal models, accurate and comprehensive functional testing is not only important to determine whether a novel therapeutic approach is successful but is also indispensable for understanding complex CNS processes such as the mechanisms leading to spontaneous recovery[1,2]. In neuroscience research, models based on rodents are commonly used, and locomotion is one of the most frequently investigated motor functions[3–5].

For evaluation of locomotor deficits, various readouts such as endpoint measures[6,7] (scores), biomechanical measures[8–10] (kinematics and kinetics) or electromyography (EMG)[9,11] are commonly used. However, these readouts suffer from several limitations. The most commonly used scores are neither linear nor objective and often have a low sensitivity, especially with regard to treatment effects or compensatory strategies[4,12]. Established scoring systems are generally developed for a particular type of injury and thus are not easily transferred to other models[7]. Highly sensitive biomechanical measurements or EMG recordings usually focus on a few very specific aspects of a movement, for example joint angles or timing of muscle activity, whereas other aspects, such as changes in body posture, are rarely assessed. As the overall functional status of the animal is often ignored, data obtained from these approaches can be difficult to interpret[12]. Furthermore, application of these methods is limited mainly to a few specialized laboratories. The use of several endpoint measures combined with quantitative biomechanical readouts has been emphasized in the literature as a priority and might help overcome some of the above-mentioned problems, but this is usually expensive, time- and space-consuming, and not standardized, hindering comparison of results between laboratories[4,12]. Adding an additional level of difficulty to the behavior analysis, rodents show various forms of locomotion depending on their environment. This includes skilled walking, normal walking on even ground or, in an aquatic environment, wading through shallow water or swimming. These types of locomotion differ considerably with regard to the motor pattern produced, sensory input and participating CNS networks[13–16] and, therefore, might be differentially affected by a given CNS injury. Thus, a comprehensive analysis of the animals' behavior, including different forms of locomotion, is necessary for a full assessment of the consequences of a lesion and is a prerequisite to linking neuroanatomical changes with functional outcome. However, studies investigating the effects of a given CNS injury by assessing full, quantitative locomotor profiles are lacking.

The objective of this study was to undertake a systematic and comprehensive evaluation of the effects of various insults to the CNS using four motor tasks that test different aspects of locomotion in rats and mice. By assessing a number of objective and quantitative outcome measures, we generated locomotor profiles characteristic for the investigated models of CNS damage. Thus, the data set presented here can guide the selection of the appropriate lesion paradigm and the corresponding outcome measures for future animal studies.

[1]Brain Research Institute, University and ETH Zurich, Zurich, Switzerland. [2]Spinal Cord Injury Center, Balgrist University Hospital, Zurich, Switzerland. [3]These authors contributed equally to this work. Correspondence should be addressed to B.Z. (zoerner@hifo.uzh.ch).

RECEIVED 27 JANUARY; ACCEPTED 25 JUNE; PUBLISHED ONLINE 15 AUGUST 2010; DOI:10.1038/NMETH.1484

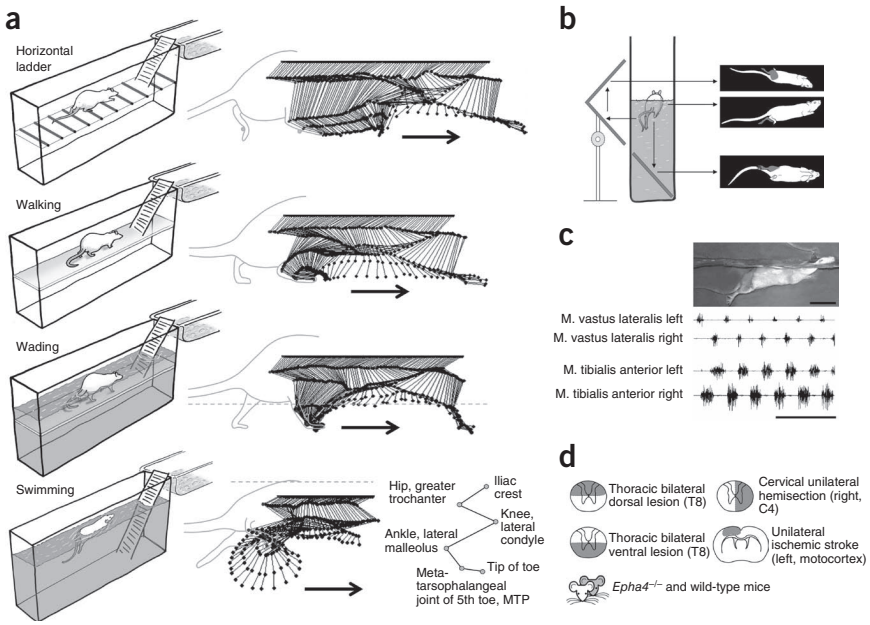

Figure 1 | Experimental setup for detailed evaluation of locomotor function in rodents after different forms of CNS damage. (**a**) We tested locomotion in four different behavioral tasks by introducing different elements (horizontal ladder, shelf, water) into a basin. Tasks evaluated are walking over an irregular horizontal ladder, overground locomotion, wading through shallow water and swimming. Stick diagrams of a single hindlimb step or swim cycle obtained from an uninjured rat illustrate that movement patterns differ considerably between tasks. Arrows indicate direction of movement and dashed line illustrates water level during wading and swimming. Bony landmarks for kinematic analysis of hindlimb movements are shown. (**b**) An arrangement of three mirrors enables recording of the performance with a high-speed camera from the left, right and bottom views, simultaneously. (**c**) Photograph of a swimming rat with head adaptor for EMG recordings. Scale bar, 5 cm. Sequences of amplified EMG show hindlimb muscle activity of an uninjured rat during swimming. M., musculus; scale bar, 500 ms. (**d**) Schematic representations illustrate paradigms of CNS damage evaluated in this study. CNS injuries are either bilateral dorsal spinal lesions at thoracic vertebral level 8 (T8), bilateral ventral spinal lesions at T8, unilateral right-sided spinal hemisections at cervical level 4 (C4) or ischemic strokes in the left motor cortex. *Epha4*-knockout mice (*Epha4*$^{-/-}$) are compared to wild-type mice.

RESULTS

Setup for locomotor testing in rodents

We evaluated locomotor function in rats and mice in a rectangular Plexiglas basin (**Supplementary Fig. 1a**). By changing the conditions within the basin, we investigated four different types of locomotion (**Fig. 1a**). To test skilled locomotion, we used a horizontal ladder. For assessment of overground locomotion, we replaced the ladder with a Plexiglas runway. For wading, we filled the basin with water to 3 cm (rats) or 1 cm (mice) above the runway's surface, because we found that these water levels were adequate to provide weight support for impaired rats without eliciting swimming movements. Finally, we evaluated swimming after filling the entire basin with water. We were able to test a single rat or mouse in all four locomotor tasks within 15 min. Three mirrors were arranged inside and outside of the basin such that the animal's performance was recorded simultaneously from three sides (left, right and below) with one camera (**Fig. 1b**). We used a color-based tracking software for automatic tracking of markers tattooed on the rat or mouse's skin overlying anatomical landmarks (**Fig. 1a**). In addition, it was possible to perform EMG recordings during the locomotor tasks (**Fig. 1c**). A large number of parameters describing locomotor outcome could be assessed in the four different tasks, as summarized in **Table 1**. However, for efficient analysis of locomotor ability, we chose a set of the most relevant parameters for each locomotor task (**Table 1**). Precise paw placement[17] and forelimb-hindlimb coordination[14] were evaluated on the horizontal ladder, whereas basic aspects of locomotor function were assessed during normal walking or wading. In addition, during wading, rats and mice tended to raise themselves as much as possible out of the water, thus maximally extending their limbs. Therefore, we assessed body height and joint angles in this task and interpreted them as measures of strength. During swimming, rats and mice showed consistent, stereotypical hindlimb movements and wave-like tail movements, which allowed reliable kinematic assessment of different forms of coordination and movement patterns.

Evaluation of locomotor impairments

To model different types of CNS injury, adult female Lewis rats received surgical dorsal thoracic, ventral thoracic or unilateral right-sided cervical spinal cord injuries (SCI) or unilateral left-sided ischemic strokes in the motor cortex induced by stereotactic injections of endothelin-1, a potent vasoconstrictor (**Fig. 1d**). We also assessed locomotion in a genetically modified mouse line, Eph receptor A4–knockout (*Epha4*$^{-/-}$), with a characteristic hopping gait[18] and compared them to wild-type mice.

In the horizontal ladder task, trained intact rats (**Fig. 2a**) and mice crossed the ladder almost without slips or missteps, and hindlimbs were always placed on the rung that was previously occupied by the ipsilateral forepaw, indicating perfect coordination of fore- and hindlimbs. After bilateral dorsal thoracic SCI, rats showed significant deficits in accurate hindpaw placement, typically owing to short targeting ($P < 0.0001$, one-way repeated-measures ANOVA, $n = 5$ rats; **Fig. 2b**,**c**). Rungs used by the ipsilateral forepaw were less frequently targeted by the respective hindlimb (49 ± 14%, 3 d after injury, group mean ± s.e.m., $n = 5$ rats), suggesting impaired fore-hindlimb coordination (**Fig. 2d**). No substantial recovery of either skill was detected at 28 d after injury. Rats with thoracic bilateral ventral SCI or cervical hemisections had very low performance on the ladder; precise hindpaw placement and fore-hindlimb coordination were virtually absent post-injury (not shown). After cervical hemisection, the ipsilesional forelimb was strongly impaired and only passively dragged over the rungs. Left cortical strokes resulted in slight and transitory but significant deficits in skilled placement of the right fore- and hindpaw (forepaw, $P = 0.0122$; hindpaw, $P = 0.0344$; one-way repeated-measures ANOVA, $n = 3$ rats), whereas left limbs were unimpaired (**Fig. 2e**). Fore-hindlimb coordination was

Table 1 | Parameters of locomotor function

Parameter	Measure	Horizontal ladder	Walking	Wading	Swimming
General locomotor function					
Velocity of locomotion	m s^{-1}	+	+	+	+
Trunk instability	s, cm	+	+	+	+
Body height, body angle	cm, degrees	+	++ (**Fig. 3g**)	++ (**Fig. 4b,e,g**)	+
Duration of tail or abdominal dragging	s	+	+	+	–
Base of support (distance between paws)	cm	+	++ (**Fig. 3b**)	+	+
Forelimb activity during swimming	no. FL strokes per run	–	–	–	++ (**Fig. 5b**)
Tail position, tail height, tail movement pattern, tail oscillation, tail motion velocity	cm, s^{-1}, cm s^{-1}	+	+	+	++ (**Fig. 5i,h**)
Basic and skilled limb movement					
Correct stepping, accurate paw placement	% plantar or functional steps	++ (**Fig. 2b,c,e,g**)	+	+	–
Step or swim cycle duration, phase duration	s	+	+	+	+
Linear displacement (for example, limb pro- and retraction, step height)	cm	+	++ (**Fig. 3d**)	++ (**Fig. 4d,f**)	+
Angular displacement (for example, range of motion, minimal and maximal joint angles)	degrees	+	+	++ (**Fig. 4b**)	+
Velocity or acceleration of displacement	cm s^{-1}, radian s^{-1}, cm s^{-2}, radian s^{-2}	+	+	+	++ (**Fig. 5c**)
Toe clearance (paw dragging)	% steps with paw dragging, % of step cycle duration	+	++ (**Fig. 3f**)	++ (**Fig. 4c**)	–
Paw position and rotation	cm, degrees	+	++ (**Fig. 3c**)	+	+
Coordination					
FL-HL coordination					
Coordinated placement of fore- and hindpaws on ladder	% identical rungs targeted	++ (**Fig. 2d,f,h**)	–	–	–
Ratio of FL and HL cycle duration	s s^{-1}	+	++ (**Fig. 3e**)	+	–
Phase dispersion, footfall diagram	% deviation	+	+	+	–
Left-right coordination					
Ratio of left and right limb cycle duration	s s^{-1}	+	+	+	+
Phase dispersion, footfall or phase diagram, polar plot	% deviation	+	++ (**Fig. 3h**)	+	++ (**Fig. 5d,e**)
Timing of muscle activity (EMG recordings)	s	+	+	+	++ (**Fig. 1c**)
Intralimb coordination					
Timing of joint excursions	s	+	+	+	+
Limb motion patterns (for example, stick diagram, spatial displacement plot, angle-angle plot)	cm, degrees	+	+	+	++ (**Fig. 5f,j**)
Timing of muscle activity (EMG recordings)	s	+	+	+	++ (**Fig. 1c**)
Tail-HL coordination					
Timing of hindlimb excursions in relation to tail motion	s	+	+	+	++ (**Fig. 5g**)
Intratail coordination					
Timing of motion of different tail segments	s	–	–	–	+

(–) parameter not applicable or measurable; (+) parameter measurable; (++) recommended outcome parameter. HL, hindlimb; FL, forelimb.

unchanged after unilateral strokes (**Fig. 2f**). When crossing the horizontal ladder, the *Epha4*$^{-/-}$ mice showed no impairment of precise paw placement (**Fig. 2g**). *Epha4*$^{-/-}$ mice had synchronous steps with both forelimbs and hindlimbs, whereas fore- hindlimb coordination was normal (**Fig. 2h**).

During overground walking (**Fig. 3a**), rats with dorsal thoracic SCI consistently showed weight-bearing steps. However, the gait was unstable, leading to a significantly increased base of support (P = 0.0275, one-way repeated-measures ANOVA, n = 5 rats; **Fig. 3b**) and increased hindpaw exorotation (P = 0.0002, one-way repeated-measures ANOVA, n = 5 rats; **Fig. 3c**). Kinematic analysis revealed a significant backwards shift of hindlimb excursions although the total extent of movement remained unchanged (protraction, P = 0.0008; retraction, P = 0.0041; total, P = 0.6693; one-way repeated-measures ANOVA, n = 5 rats; **Fig. 3d**). In addition, fore-hindlimb coordination (P = 0.0003, one-way repeated-measures ANOVA, n = 5 rats; **Fig. 3e**) and toe clearance (P < 0.0001, one-way repeated-measures ANOVA; 70 ± 12% of steps with paw dragging, 3 days after injury, group mean ± s.e.m., n = 5 rats; **Fig. 3f**) was significantly impaired. Seven days after either ventral thoracic lesions or cervical hemisections, the walking pattern of the hindlimbs was massively impaired. After ventral injury, weight-bearing hindlimb steps were extremely rare, and limbs were maximally extended with limb excursions reduced to about 1 cm (**Fig. 3d**). Rats dragged themselves over the runway with their forelimbs, with minimal hindlimb movements, thus making more detailed analysis of hindlimb function almost impossible. The flat position was reflected by a reduced height of the iliac crest (**Fig. 3g**). However, total hindlimb excursions and limb protraction substantially improved within 4 weeks (**Fig. 3d**). Rats with a stroke walked almost normally, with only a tendency toward an increased external rotation of the right hindpaw (not shown). Overground walking in *Epha4*$^{-/-}$ mice was characterized by synchronous hindlimb movements (**Fig. 3h**). Coupling between the forelimbs was also observed when mice walked at a constant speed but not during exploration (**Fig. 3h**).

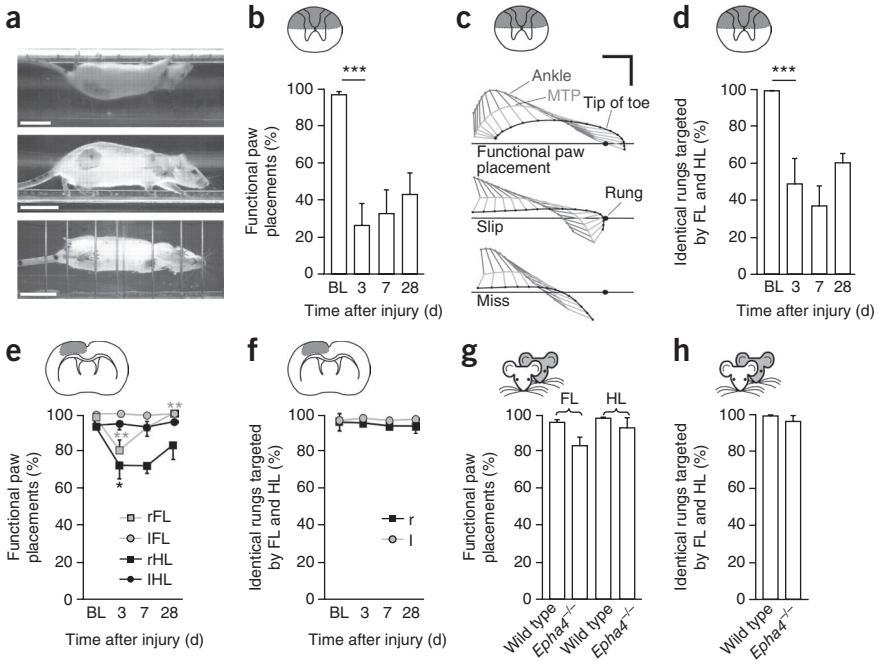

Figure 2 | Skilled locomotion after CNS damage. We evaluated skilled walking before (baseline, BL) and at several time points after dorsal thoracic SCI (n = 5 rats) or unilateral left-sided cortical stroke (n = 3 rats). Schematic representations illustrate paradigms of CNS damage (**Fig. 1d**). (**a**) Image of intact rat crossing horizontal ladder. Scale bars, 5 cm. (**b**) Precise placement of hindpaws after dorsal SCI. (**c**) Stick diagrams based on tracking of the ankle, metatarsophalangeal joint of fifth toe (MTP) and tip of toe illustrate typical hindpaw steps classified as functional paw placement, slip or miss, after dorsal SCI; scale bars, 2 cm. (**d**) Fore-hindlimb coordination after dorsal SCI. FL, forelimb; HL, hindlimb. (**e**,**f**) Precise placement of fore- and hindpaws (**e**) and fore-hindlimb coordination (**f**) after stroke. (**g**,**h**) Precise placement of fore- and hindpaws (**g**) and fore-hindlimb coordination (**h**) in wild-type (n = 3 mice) and *Epha4*$^{-/-}$ mice (n = 3 mice) assessed in a single testing session. Bar and line graphs in **b**,**d**–**h** show group mean values for every testing session. In **b**,**d**,**g**,**h**, values for left and right body side are averaged; in **e**,**f**, separate values for left (l) and right (r) side are presented. For differences between time points in **b**,**d**–**f**, one-way repeated-measures ANOVA followed by *post hoc* Bonferroni tests were performed. For differences between mice lines in **g**,**h**, data was subjected to Student's t-test (two-tailed, unpaired). $^{**}P < 0.01$, $^{***}P < 0.001$ indicate significantly different performances. Error bars, s.e.m.

During wading in intact rats and mice, characteristic aspects of the locomotor pattern were a tiptoeing gait, elevated body position and increased limb excursions (**Fig. 4a**). After dorsal SCI and unilateral stroke, only minor lesion deficits were observed; the tiptoeing gait disappeared and heels touched the ground in the stance phase. Body height and joint angles of the knee and ankle, but not the hip, were transitorily reduced after dorsal SCI (**Fig. 4b**). Iliac crest height and joint angles of knee and ankle were strongly correlated (r_{knee} = 0.87, r_{ankle} = 0.91, Pearson's correlation coefficients, n = 88 steps of five rats, obtained 3, 7 and 28 d after injury). In contrast to normal overground walking, base of support was unchanged (data not shown), paw dragging occurred only occasionally (38 ± 14% of steps with paw dragging, 3 d after injury, group mean ± s.e.m., n = 5 rats; **Fig. 4c**), and hindlimb protraction was not significantly changed (P = 0.4883, one-way repeated-measures ANOVA, n = 5 rats; **Fig. 4d**). Rats with ventral

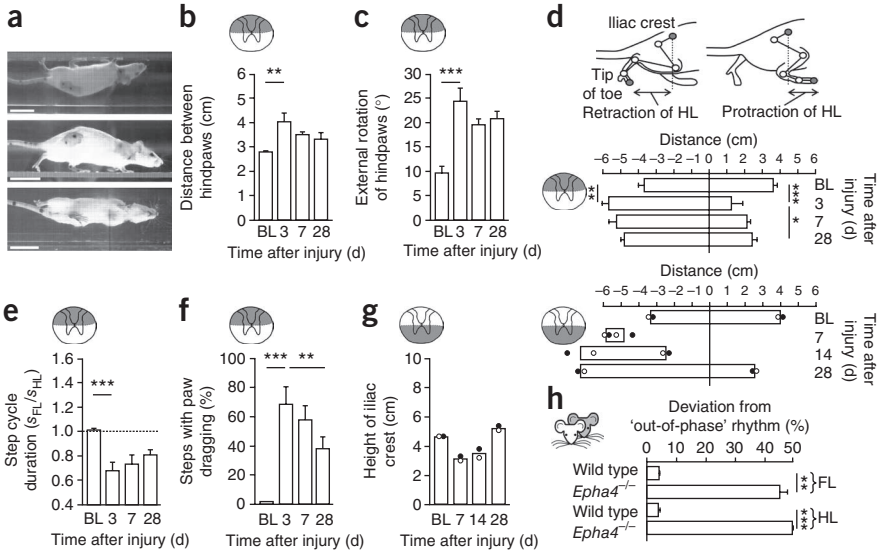

Figure 3 | Overground walking after CNS damage. Walking was tested before (baseline, BL) and at several time points after dorsal thoracic (n = 5 rats) or ventral thoracic SCI (n = 2 rats). Schematic representations illustrate paradigms of CNS damage (**Fig. 1d**). (**a**) Image of intact rat walking over runway; scale bars, 5 cm. (**b**,**c**) Base of support (**b**) and external rotation of hindpaws at initial ground contact (**c**) after dorsal SCI. (**d**) Horizontal hindlimb (HL) excursions described via the maximal protraction (maximal x-value) and retraction (minimal x-value) of the toe relative to the iliac crest after dorsal (upper graph) and ventral (lower graph) SCI. (**e**,**f**) Fore-hindlimb coordination (**e**) and toe clearance (**f**) after dorsal SCI. (**g**) Height of iliac crest at mid-stance phase after ventral SCI. (**h**) Deviation from perfect left-right alternation (out of phase) of fore- and hindlimbs in wild-type (n = 3 mice) and *Epha4*$^{-/-}$ mice (n = 3 mice) assessed in one testing session. Bars in **b**–**h** represent group mean values for every testing session. In lower graph of **d** and in **g**, results for individual rats are shown; black and white dots represent individual rats; data were not subjected to statistical testing. For differences between time points in **b**,**c**,**e**,**f** and upper graph of **d**, one-way repeated-measures ANOVA followed by *post hoc* Bonferroni tests were performed. For differences between mice lines in **h**, Student's t-test (two-tailed, unpaired) was applied. $^{*}P < 0.05$, $^{**}P < 0.01$, $^{***}P < 0.001$ indicate significantly different performances. Error bars, s.e.m.

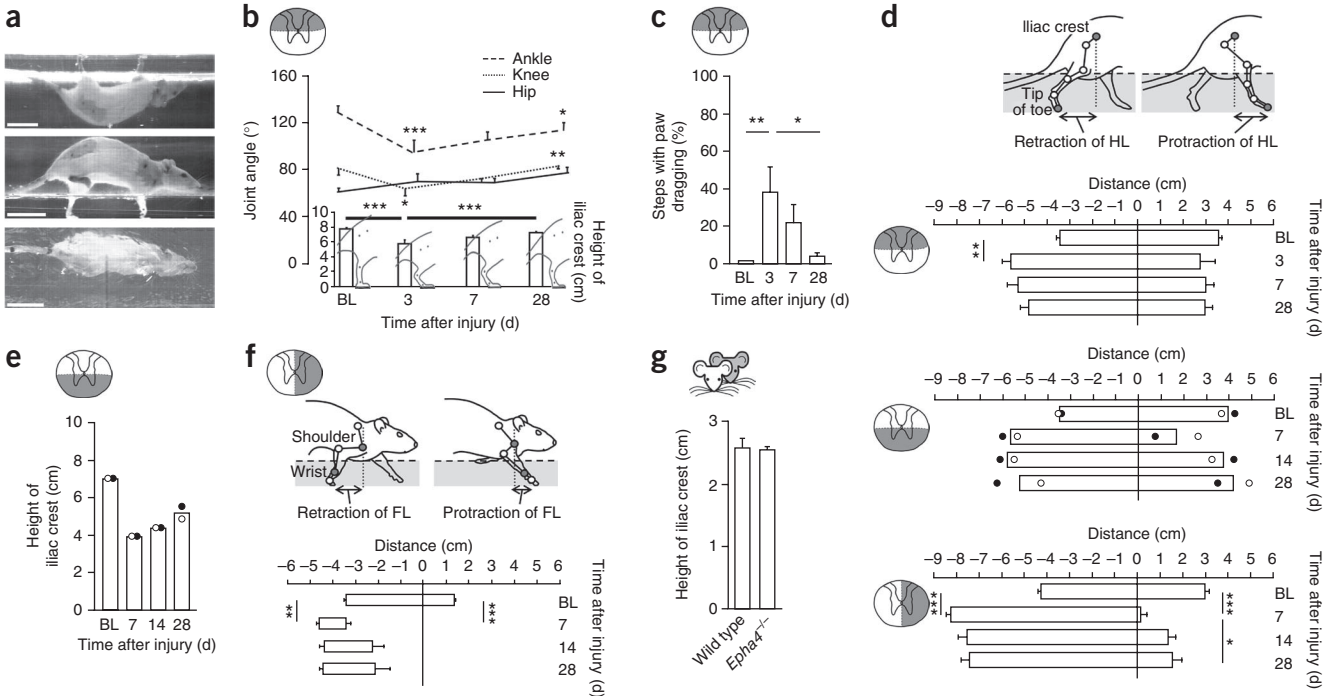

Figure 4 | Wading after CNS damage. Wading through shallow water was assessed before (baseline, BL) and at several time points after dorsal thoracic (n = 5 rats), ventral thoracic (n = 2 rats) or unilateral right-sided cervical SCI (n = 4 rats). Schematic representations illustrate paradigms of CNS damage (**Fig. 1d**). (**a**) Image of intact rat wading; scale bars, 5 cm. (**b**) Hindlimb joint angles and iliac crest height at mid-stance phase after dorsal SCI. (**c**) Toe clearance in rats with dorsal SCI. (**d**) Horizontal hindlimb (HL) excursions during wading are presented as in **Figure 3d** for rats with dorsal (upper graph), ventral (middle graph) and unilateral cervical SCI (lower graph, ipsilesional hindlimb). (**e**) Height of iliac crest at mid-stance phase after ventral SCI. (**f**) Horizontal excursions of ipsilesional forelimb (FL) after unilateral cervical SCI. (**g**) Iliac crest height at mid-stance phase in wild-type (n = 3 mice) and *Epha4*$^{-/-}$ mice (n = 3 mice) measured at a single time point. Bars in **b**–**g** represent group mean values for every testing session. In **d** middle graph and in **e**, results for individual rats are shown; black and white dots represent individual rats; no statistical testing was performed. For differences between time points in **b**,**c**,**f**, and upper and lower panels of **d**, one-way repeated-measures ANOVA and *post hoc* Bonferroni tests were applied. For differences between mouse lines in **g**, Student's t-test (two-tailed, unpaired) was used. *P < 0.05, **P < 0.01, ***P < 0.001 indicate significantly different performances. Error bars, s.e.m.

thoracic lesions or with unilateral cervical injuries produced weight-bearing hindlimb steps as early as 7 d after injury during wading, even though steps were characterized by increased retraction and reduced protraction (**Fig. 4d**). After ventral injury, a gradual increase in iliac crest height during the recovery process was observed (**Fig. 4e**). After unilateral cervical hemisection, ipsilesional forelimb excursions were strongly impaired (**Fig. 4f**), paralleled by a strong reduction in the range of motion in the shoulder and elbow joint (data not shown). The *Epha4*$^{-/-}$ mice showed a hopping gait during wading as well as during walking. Other parameters such as iliac crest height at mid-stance phase were unchanged in the mutant (**Fig. 4g**).

Swimming is a stereotypical form of locomotor behavior characterized by powerful hindlimb strokes that are performed in a very consistent and well-coordinated manner, providing the main drive for forward motion, while forepaws are usually immobile below the chest (**Fig. 5a**)[19]. The horizontal sinusoidal oscillations of the tail and occasional forelimb strokes are probably important for navigation and stability during swimming. In infant rats[20] and after SCI in adults[21], extensive use of the forelimbs has been interpreted as a compensatory strategy for immature or impaired hindlimb function, respectively. Accordingly, we found that the number of forelimb strokes was significantly increased after dorsal thoracic SCI (P = 0.0098, one-way repeated-measures ANOVA, n = 5 rats; **Fig. 5b**). Hindlimb movements were slower, as indicated by significantly reduced peak toe velocities (P = 0.001, one-way repeated-measures ANOVA, n = 5 rats) and longer stroke-cycle durations with extended power and return stroke phases (**Fig. 5c**,**d**). A transient disturbance of left-right coordination was present, and hindlimb excursions were initially smaller and of irregular shape (**Fig. 5d**–**f**). Hindlimb function during swimming recovered impressively, which was reflected in most of the parameters assessed. In contrast, the strongly impaired tail-hindlimb coordination, tail movement velocity and tail motion patterns did not improve over time (**Fig. 5g**–**i**). Throughout the testing period, rats with ventral thoracic SCI showed massive impairments in hindlimb (**Fig. 5f**) and tail function (data not shown) and strong lateral instability in the swimming task. Forward motion was achieved only by excessive forelimb use. After cervical hemisection, kinematic analysis showed transiently exaggerated joint excursions of the ipsilesional hindlimb (**Fig. 5f**). Tail movements were slower and strongly deviated toward the uninjured side (**Fig. 5h**,**i**), suggesting an imbalance of tail muscle activity in favor of the intact side. Accordingly, rats with cervical hemisections suffered from lateral instability during swimming. After unilateral stroke, no deficits in swimming were detected (data not shown). *Epha4*$^{-/-}$ mice showed consistent coupling of hindlimbs, resulting in an uneven, bumpy swimming style that appeared less efficient than the regular left-right alternating pattern of wild-type mice. A shift in the angle-angle plots toward

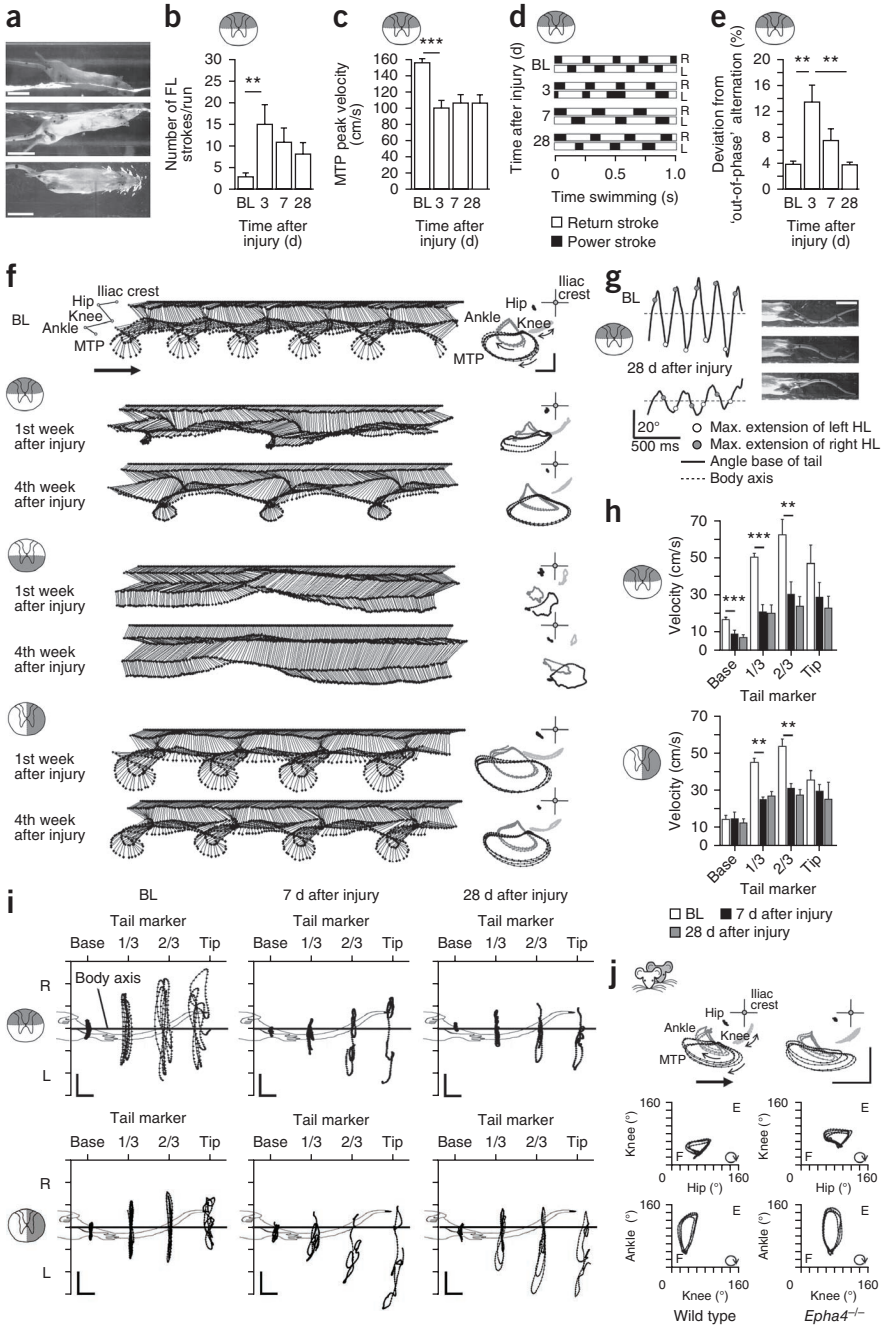

Figure 5 | Swimming after CNS damage. Swimming was tested before (baseline, BL) and at several time points after dorsal thoracic (n = 5 rats), ventral thoracic (n = 2 rats) or unilateral right-sided cervical SCI (n = 4 rats). Schematic representations illustrate paradigms of CNS damage (**Fig. 1d**). (**a**) Intact rat swimming; scale bars, 5 cm. (**b**,**c**) Forelimb (FL) strokes (**b**) and peak velocity of metatarsophalangeal joint (MTP; **c**) after dorsal SCI. (**d**) Phase diagram illustrating left-right alternation of hindlimbs after dorsal SCI. R, right; L, left. (**e**) Deviation from perfect hindlimb alternation (out of phase) after dorsal SCI. (**f**) Stick diagrams and spatial displacement plots illustrate swimming performance after dorsal, ventral or unilateral SCI over a period of 1 s. Thick arrows, swimming direction; thin arrows, temporal progression of movements; scale bars, 2 cm. (**g**) Disturbed synchrony of tail base excursions and hindlimb (HL) extension after dorsal SCI. (**h**) Mean movement velocity of tail markers (base, first third, second third, tip of tail) after dorsal and unilateral SCI; scale bar, 5 cm. (**i**) Lateral movements of tail markers over a period of 1 s after dorsal and unilateral SCI; scale bars, 2 cm. (**j**) Spatial displacement and angle-angle plots of an *Epha4*$^{-/-}$ mouse and a wild-type mouse; scale bars, 2 cm. E, Extension; F, Flexion. Bars in **b**,**c**,**e**,**h** represent group mean values for every testing session; one-way repeated-measures ANOVA and *post hoc* Bonferroni tests; $^{**}P < 0.01$, $^{***}P < 0.001$. Error bars, s.e.m. **d**,**f**,**g**,**i** show results of single rats, and **j** of single mice, representative for their experimental group.

higher degrees indicated increased extension of the hip and knee joint (**Fig. 5j**). In addition, *Epha4*$^{-/-}$ mice showed an extensive and coupled use of both forelimbs during swimming.

DISCUSSION

We used physiological, objective and quantitative parameters to generate comprehensive locomotor profiles for some of the most common models of CNS insult. We found that these profiles were highly dependent on lesion type and severity. Some parameters were more sensitive to, or more affected by, one particular lesion than another, allowing for the selection of suitable combinations of locomotor task, readouts and lesion type in future studies.

After dorsal thoracic SCI, rats performed weight-bearing hindlimb steps and showed only transitory deficits in left-right and intralimb coordination during swimming, indicating that the lumbar spinal central pattern generator (CPG) networks and their main modulatory inputs were unaffected by the injury[22,23]. However, damage to major components of the cortico- and rubrospinal tract and the gracile fasciculus led to strongly impaired paw placing, seen during skilled walking and overground locomotion, with respect to accuracy, strength and velocity. This suggests that these tracts are important in skilled and distal hindlimb motor function in rats[17]. In addition, after this lesion type fore-hindlimb coordination and tail movements were also impaired, possibly owing to damage of components of the propriospinal system[24] and bulbospinal tracts, respectively. In line with these findings, unilateral strokes comprising the fore- and hindlimb sensorimotor region resulted in contralateral deficits in fine motor control without affecting other basic aspects of locomotion during swimming, walking or wading. Ventral thoracic SCIs disrupt, among other systems, vestibulospinal fibers and main portions of the reticulo- and raphespinal tracts. The latter are known to be crucial for the initiation and modulation of stepping movements via CPG networks[25,26]. Accordingly, in the first week after injury rats were not able to perform hindlimb swimming strokes

or stepping movements during normal overground walking. Rats could generate hindlimb movements in the wading test, as assistive weight support was provided by the water buoyancy. Although stepping ability improved substantially over time, rats were, even after several weeks, barely able to produce hindlimb strokes during swimming. In the absence of major bulbospinal input, it can be assumed that the rhythmic hindlimb movements generated by the lumbar CPGs rely on or are facilitated by proproiceptive input owing to limb loading that is present during wading but not during swimming[27]. Thus, as both proproiceptive input and some weight support seem to be required for hindlimb movements after this lesion, wading is the most appropriate test to demonstrate and evaluate locomotor ability in these rats. After cervical unilateral hemisection, fore- and hindlimbs were differently affected in the four different tasks. Forelimb locomotor function was extremely poor throughout the entire testing period in all locomotor tasks. In contrast, hindlimb movements were present during wading and swimming within the first week of injury, followed by substantial functional recovery indicated by regular weight-bearing hindlimb steps and excellent intralimb coordination. However, rats remained poor in their ability to cross the ladder. These data suggest that the descending fiber tracts in the spared hemicord were at least partially sufficient to compensate for lost supraspinal input. This partial compensation allowed for good basic locomotor function of the affected hindlimb but not forelimb during walking, wading and swimming; however, it did not enable skilled movements of either limb. The absence of EphA4, an important axon guidance receptor during development, led to anatomical alterations of corticospinal projections and locomotor networks in the lumbar spinal cord[18,28]. These changes are considered responsible for the previously described synchronous hindlimb movements ('hopping') during walking[18]. Additionally, we found that forelimb movements were synchronously coupled during overground locomotion. No deficit in precise paw placement was detected on the horizontal ladder. These behavioral data suggest that important anatomical changes are also present on the level of cervical CPG networks[29] but that the anatomically altered corticospinal system is able to control precise targeted movements. These conclusions were based on testing in several locomotor tasks, highlighting the importance of broad screening.

Our data were comprehensive in several ways. We provided information about whether and how a task was performed after a variety of CNS insults in rats and mice. The battery of readouts used ranged from very basic to very specific. We assessed movements of all relevant body parts (forelimbs, hindlimbs, trunk and tail) as well as the most important characteristics of locomotion—for example, different forms of coordination. In addition, our analysis was highly sensitive, as it was able to detect compensatory strategies; for example, we observed that during swimming, slower, less powerful and uncoordinated hindlimb strokes were compensated for by extensive forelimb use and exaggerated hindlimb movements in rats with SCI. A number of established as well as novel parameters were assessed. For the established parameters, our results are in line with data from earlier studies using comparable lesion types and testing conditions[16,17,21,30]. In this study, we concentrated on commonly used CNS injury paradigms in adult rats and on one transgenic mouse line. However, our method is not limited to these situations and could also be used to study models of peripheral nerve injury, muscular diseases, and neuroinflammatory or neurodegenerative diseases.

Our results, derived from a systematic evaluation of different types of CNS damage in rodents, emphasize the importance of detailed locomotor profiling in animal research. Broad application of these sets of objective and quantitative readouts will improve and standardize behavioral assessment.

METHODS

Methods and any associated references are available in the online version of the paper at http://www.nature.com/naturemethods/.

Note: Supplementary information is available on the Nature Methods website.

ACKNOWLEDGMENTS

We dedicate this work to the memory of our late colleague and friend Eva Hochreutener, who contributed excellent graphical work and suggestions essential to this study. We thank R. Schöb and P. Scheuble for IT support and S. Giger for construction of the behavioral testing system, L. Schnell for her pioneering work on behavior testing and evaluation in our laboratory, M. Petrinovic for help with mouse testing, R. Klein (Department of Molecular Neurobiology, Max Planck Institute of Neurobiology, Martinsried) for providing the *Epha4*$^{-/-}$ mice and members of the software company ALEA Solutions GmbH for close collaboration and for the development of the tracking software. This study was supported by grants of the Swiss National Science Foundation (31-63633.00 and 3100A0-122527/1), the National Centre for Competence in Research 'Neural Plasticity and Repair' of the Swiss National Science Foundation, the Spinal Cord Consortium of the Christopher and Dana Reeve Foundation and the Framework Program 7 EU Collaborative Project Spinal Cord Repair.

AUTHOR CONTRIBUTIONS

B.Z. and L.F. designed the study, developed the testing setup, performed surgeries, collected and analyzed data, made the figures and prepared the manuscript. M.L.S. developed stroke lesions, performed surgeries and prepared the manuscript. R.G. developed the EMG setup, performed the recordings and collected and analyzed data. H.K. developed the testing setup and developed software. M.R. performed surgeries and collected and analyzed data. M.B. developed software and collected and analyzed data. M.E.S. designed the study, prepared the manuscript, and conceived and supervised the study.

COMPETING FINANCIAL INTERESTS

The authors declare competing financial interests: details accompany the full-text HTML version of the paper at http://www.nature.com/naturemethods/.

Published online at http://www.nature.com/naturemethods/.
Reprints and permissions information is available online at http://npg.nature.com/reprintsandpermissions/.

1. Basso, D.M. Neuroanatomical substrates of functional recovery after experimental spinal cord injury: implications of basic science research for human spinal cord injury. *Phys. Ther.* **80**, 808–817 (2000).
2. Raineteau, O. & Schwab, M.E. Plasticity of motor systems after incomplete spinal cord injury. *Nat. Rev. Neurosci.* **2**, 263–273 (2001).
3. McEwen, M.L. & Springer, J.E. Quantification of locomotor recovery following spinal cord contusion in adult rats. *J. Neurotrauma* **23**, 1632–1653 (2006).
4. Muir, G.D. & Webb, A.A. Mini-review: assessment of behavioural recovery following spinal cord injury in rats. *Eur. J. Neurosci.* **12**, 3079–3086 (2000).
5. Metz, G.A., Merkler, D., Dietz, V., Schwab, M.E. & Fouad, K. Efficient testing of motor function in spinal cord injured rats. *Brain Res.* **883**, 165–177 (2000).
6. Kunkel-Bagden, E., Dai, H.N. & Bregman, B.S. Methods to assess the development and recovery of locomotor function after spinal cord injury in rats. *Exp. Neurol.* **119**, 153–164 (1993).
7. Basso, D.M., Beattie, M.S. & Bresnahan, J.C. A sensitive and reliable locomotor rating scale for open field testing in rats. *J. Neurotrauma* **12**, 1–21 (1995).
8. Hamers, F.P., Lankhorst, A.J., van Laar, T.J., Veldhuis, W.B. & Gispen, W.H. Automated quantitative gait analysis during overground locomotion in the

rat: its application to spinal cord contusion and transection injuries. *J. Neurotrauma* **18**, 187–201 (2001).
9. Courtine, G. *et al.* Transformation of nonfunctional spinal circuits into functional states after the loss of brain input. *Nat. Neurosci.* **12**, 1333–1342 (2009).
10. Magnuson, D.S. *et al.* Swimming as a model of task-specific locomotor retraining after spinal cord injury in the rat. *Neurorehabil. Neural Repair* **23**, 535–545 (2009).
11. Gorska, T., Chojnicka-Gittins, B., Majczynski, H. & Zmyslowski, W. Recovery of overground locomotion following partial spinal lesions of different extent in the rat. *Behav. Brain Res.* **196**, 286–296 (2009).
12. Basso, D.M. Behavioral testing after spinal cord injury: congruities, complexities, and controversies. *J. Neurotrauma* **21**, 395–404 (2004).
13. Roy, R.R., Hutchison, D.L., Pierotti, D.J., Hodgson, J.A. & Edgerton, V.R. EMG patterns of rat ankle extensors and flexors during treadmill locomotion and swimming. *J. Appl. Physiol.* **70**, 2522–2529 (1991).
14. Bolton, D.A., Tse, A.D., Ballermann, M., Misiaszek, J.E. & Fouad, K. Task specific adaptations in rat locomotion: runway versus horizontal ladder. *Behav. Brain Res.* **168**, 272–279 (2006).
15. Garnier, C., Falempin, M. & Canu, M.H. A 3D analysis of fore- and hindlimb motion during locomotion: comparison of overground and ladder walking in rats. *Behav. Brain Res.* **186**, 57–65 (2008).
16. Kanagal, S.G. & Muir, G.D. Task-dependent compensation after pyramidal tract and dorsolateral spinal lesions in rats. *Exp. Neurol.* **216**, 193–206 (2009).
17. Metz, G.A. & Whishaw, I.Q. Cortical and subcortical lesions impair skilled walking in the ladder rung walking test: a new task to evaluate fore- and hindlimb stepping, placing, and co-ordination. *J. Neurosci. Methods* **115**, 169–179 (2002).
18. Dottori, M. *et al.* EphA4 (Sek1) receptor tyrosine kinase is required for the development of the corticospinal tract. *Proc. Natl. Acad. Sci. USA* **95**, 13248–13253 (1998).
19. Gruner, J.A. & Altman, J. Swimming in the rat: analysis of locomotor performance in comparison to stepping. *Exp. Brain Res.* **40**, 374–382 (1980).
20. Schapiro, S., Salas, M. & Vukovich, K. Hormonal effects on ontogeny of swimming ability in the rat: assessment of central nervous system development. *Science* **168**, 147–150 (1970).
21. Liebscher, T. *et al.* Nogo-A antibody improves regeneration and locomotion of spinal cord-injured rats. *Ann. Neurol.* **58**, 706–719 (2005).
22. Kiehn, O. Locomotor circuits in the mammalian spinal cord. *Annu. Rev. Neurosci.* **29**, 279–306 (2006).
23. Goulding, M. Circuits controlling vertebrate locomotion: moving in a new direction. *Nat. Rev. Neurosci.* **10**, 507–518 (2009).
24. Juvin, L., Simmers, J. & Morin, D. Propriospinal circuitry underlying interlimb coordination in mammalian quadrupedal locomotion. *J. Neurosci.* **25**, 6025–6035 (2005).
25. Grillner, S., Wallen, P., Saitoh, K., Kozlov, A. & Robertson, B. Neural bases of goal-directed locomotion in vertebrates—an overview. *Brain Res. Brain Res. Rev.* **57**, 2–12 (2008).
26. Hagglund, M., Borgius, L., Dougherty, K.J. & Kiehn, O. Activation of groups of excitatory neurons in the mammalian spinal cord or hindbrain evokes locomotion. *Nat. Neurosci.* **13**, 246–252 (2010).
27. Frigon, A. & Rossignol, S. Experiments and models of sensorimotor interactions during locomotion. *Biol. Cybern.* **95**, 607–627 (2006).
28. Butt, S.J., Lundfald, L. & Kiehn, O. EphA4 defines a class of excitatory locomotor-related interneurons. *Proc. Natl. Acad. Sci. USA* **102**, 14098–14103 (2005).
29. Yamaguchi, T. The central pattern generator for forelimb locomotion in the cat. *Prog. Brain Res.* **143**, 115–122 (2004).
30. Ghosh, A. *et al.* Functional and anatomical reorganization of the sensory-motor cortex after incomplete spinal cord injury in adult rats. *J. Neurosci.* **29**, 12210–12219 (2009).

ONLINE METHODS

Animals. We performed all experiments with the approval of and in accordance with the guidelines of the Veterinarian Office Zurich, Switzerland. CNS lesions and behavioral testing were performed on 14 adult female Lewis rats (200–250 g, Centre d'Elevage R. Janvier). In addition, we evaluated locomotor function in three Eph receptor A4 knockout (*Epha4*$^{-/-}$, C57BL/6 background, provided by R. Klein, Max Planck Institute of Neurobiology) and three wild-type C57BL/6 mice. Mice were 4–5-months-old and of both sexes. Rats and mice were housed in groups of three to five per cage, in 12:12 h light:dark cycle, with food and water *ad libitum*.

Surgery and animal care. We performed all surgeries (rats only) under general anesthesia achieved by subcutaneous injections of Hypnorm and Dormicum (Hypnorm, 120 µl per 200 g body weight, Janssen Pharmaceutics; Dormicum, 0.75 mg per 200 g body weight, Roche Pharmaceuticals). Spinal cord injuries were either a bilateral dorsal cut lesion at T8 vertebral level (n = 5 rats), a large bilateral ventral lesion at T8 (n = 2 rats) or a cervical unilateral right-sided complete hemisection at C4 (n = 4 rats). The lesions were performed as described previously[30,31]. Rats with an ischemic lesion to the cortex (stroke, n = 3 rats) received 14 stereotactic injections of the vasoconstrictor endothelin-1 (ET-1, 0.3 µg µl^{-1}; Sigma-Aldrich) into the left motor cortex (fore- and hindlimb areas). We injected a volume of 500 nl at a depth of 1.2 mm with a rate of 6 nl s^{-1}. After each injection, we left the needle in place for 3 min before it was carefully removed. After the final injection of ET-1, or after SCI, the rats were sutured and returned to a heated blanket to recover from surgery. One day before and for 2 d after surgery, rats received subcutaneous injections of analgesic (Rimadyl, 2.5 mg per kg body weight, Pfizer AG). In addition, postoperative care included daily subcutaneous injections of antibiotics (Baytril, 5 mg per kg body weight, Bayer AG) for 1 week to prevent bladder or wound infections. We checked the rats' health twice daily for the entire experiment. After SCI, bladders were manually expressed until normal bladder function returned. As expected, stroke lesions did not affect bladder function.

Testing apparatus. For evaluation and analysis of locomotor function in rats and mice, we used a single custom-designed setup, the MotoRater (**Supplementary Fig. 1a–e**). The complete setup is now commercially available at TSE-systems GmbH (http://www.tse-systems.com/). We tested the rats and mice in a clear Plexiglas basin, 150 cm long, 13 cm wide and 40 cm high (**Supplementary Fig. 1a**). At one end, a small footbridge allowed the rats and mice to exit the basin into a cage. A temperature sensor was installed to measure the water temperature. For testing of skilled locomotion, we placed into the basin a horizontal ladder (for rats, 113 cm long, 13 cm wide; for mice, 113 cm long, 7 cm wide; 15 cm above ground) with regularly (training) or irregularly (testing) spaced round metal rungs (**Supplementary Fig. 1b**). We used a Plexiglas runway (123 cm long, 13 cm wide, 15 cm above ground) to assess overground locomotion and wading (**Supplementary Fig. 1b**). For wading and swimming, the water temperature was 23 °C. Water depth for wading was 3 cm (rats) or 1 cm (mice) above the runway's surface; for swimming, water depth was 25 cm. For mice, we restricted the width of the testing corridor to 7 cm with two additional Plexiglas walls (**Supplementary Fig. 1b**). To allow evaluation of the performance from the left and right side and from below at the same time, we placed one mirror (100 cm × 16 cm) on the basin's floor at an angle of ~90° and positioned two perpendicularly arranged mirrors (100 cm × 18 cm) behind the long side of the basin (**Fig. 1b** and **Supplementary Fig. 1a,c**). We used high frame rates to film the performance in the testing basin (see below). This required an additional strong light source that was comprised of four commercially available 36-watt fluorescent lamps emitting cool white light. During testing, the lighting rack was located between the camera and the testing apparatus, illuminating the basin from above (one lamp) and below (three lamps). More detailed information is provided in **Supplementary Note 1**.

Electromyographic recordings. For EMG recordings during the locomotor tasks, we placed a cableway system on top of the basin, enabling a motile wire connection between a preamplifier and the rats' head adaptor (**Fig. 1c** and **Supplementary Fig. 1d**). Bipolar Teflon-coated stainless steel wires (Cooner Wire) were chronically implanted into the left and right musculus tibialis anterior and musculus vastus lateralis as described previously[32]. The distance between the electrode tips was 1–2 mm. Implanted wires were led subcutaneously to the head and attached to a connector that was fixed on the rat's skull with dental cement. One wire served as a ground electrode and was placed subcutaneously in the neck region of the rat. Pre-amplified signals were digitized (sampling rate of 1 kHz), amplified (1,000×) and high-pass filtered (30 Hz). We processed the data with DIAdem academic 8.1 software (National Instruments Engineering GmbH & Co. KG).

Preparation of the animals. After acclimatization to the testing apparatus, we trained the rats and mice in five daily sessions (every other day, about ten passages per animal and task) until they crossed the testing basin with a constant speed. Rats and mice were trained on the ladder with a regular arrangement of metal rungs. For testing, rung sequences were irregular and varied to avoid habituation to a particular rung pattern. Before baseline recording, the skin overlying defined anatomical landmarks on the lateral side of the forelimbs and hindlimbs was shaved and tattooed with a commercially available tattooing kit (Hugo Sachs Elektronik, Harvard Apparatus GmbH). We marked the following bony structures of the forelimb: vertebral border of the scapula (shoulder blade); tip of the humerus (shoulder joint); wrist and the fifth metacarpal head (digit)[33]. We also labeled the following hindlimb structures: iliac crest; greater trochanter (hip); lateral malleolus (ankle); metatarsophalangeal joint of fifth toe (MTP) and the tip of the toe[33]. On the ventral surface of the tail, we marked four points with tattoos: the base of the tail, the first third and second third of the tail and the tip of the tail.

Data acquisition and kinematic analysis. We tested rats with strokes and dorsal SCIs before (baseline) and 3, 7 and 28 d after injury. Locomotor performance of rats with ventral and cervical SCIs was evaluated at baseline and 7, 14 and 28 d after lesion. In these rats, we removed the early session (3 d) as rats are more severely impaired after ventral and cervical lesions than they are after stroke or dorsal SCI. We tested *Epha4*$^{-/-}$ and wild-type mice in a single session. Before every testing session, we reinforced visualization of the tattoos with a fluorescent dye (for example

fluorescent, fast-drying nail polish) or a black marker in case of albino rats. For each animal (rats and mice) and each task, we recorded three to ten passages and analyzed at least three of them. The analysis was based exclusively on video recordings captured with a high-speed color camera (Basler A504kc Color Camera, Basler AG, 1,280 × 1,024 pixels). We filmed rats and mice at a frame rate of 50, 100 or 200 frames per second (Hz) for skilled walking on the ladder, overground walking, and wading or swimming, respectively.

To increase the number of pixels per marker, we placed the camera close to the basin (distance of 100–150 cm), thereby limiting the field of view to about one-third of the length of the testing track. By moving the camera on a guide rail along the testing track, we recorded the full distance covered by the animals (**Supplementary Fig. 1e**). We attached a commercially available flashlight pointer to the camera that indicated the camera's field of view. This provided visual feedback to the experimenter, who manually moved the camera, thus allowing reliable recordings of moving rats and mice. Locomotor behavior was analyzed only in a central, 60-cm-long region of the testing apparatus to avoid artifacts owing to acceleration and deceleration at the beginning and end of the track, respectively. For each task, only passages with similar and constant movement velocities and without lateral instability (**Supplementary Note 1**) were used for kinematic analysis.

In collaboration with a software engineering company (ALEA Solutions GmbH), a color-based automated tracking software, ClickJoint version 5.0 was developed (now commercially available at ALEA Solutions GmbH) and used for offline analysis of the video recordings. For calibration of the software, we placed three 5-cm-long pieces of tape on the walls of the testing basin so they were visible from all perspectives (direct view and mirror images). As the camera was moved during recordings to follow the rats and mice on their journey through the testing basin, normalization of the spatial measurements to the position of the iliac crest (for hindlimb analysis) or the shoulder blade (for forelimb analysis) was required. The software automatically tracked, frame by frame, the markers on the skin of the rats and mice and generated two-dimensional coordinates (x, y) for every marker and time point. On the basis of these coordinates, the software modeled body segments as rigid straight lines between markers. For kinematics, movements were automatically reconstructed from changes in the marker location between consecutive frames. Angles and distances were calculated directly by the software, allowing the generation of stick diagrams and spatial displacement plots. For angle measurements, we used the smaller angle of the two alternatives; typically this was the angle at the flexor side of a limb joint. We analyzed the side and the bottom views of the rats and mice separately. Data were smoothed by applying an integrated supplementary function of the ClickJoint software using a cubic-spline function. Data were then imported into Microsoft Office Excel 2007 (Microsoft) and further analyzed with pre-assembled Excel sheets determining, for example, joint angles or distances between joints at a given time point, range of motion, coordination parameters or movement velocities. To minimize artifacts owing to divergent movements of the skin over the underlying bony structures[34], we defined the knee and elbow joints as virtual joints; that is, their positions were indirectly computed by the ClickJoint software. For the knee, the calculation was based on both the position of the markers over the hip and ankle and the length of the femur (rat = 2.5 cm, mouse = 1.3 cm) and tibia (rat = 3.5 cm, mouse = 2 cm) bones. For the elbow joint, the shoulder and wrist positions and the length of the humerus (rat = 2.5 cm, mouse = 1.1 cm) and the lower forelimb (rat = 2.8 cm, mouse = 1.2 cm) were used. For more detailed information about camera settings, software application and data processing, see **Supplementary Note 1**.

Locomotor parameters. We defined the movement phases of a limb during locomotion in accordance with the literature[9,19]. In brief, for walking and wading, a gait cycle was defined as the time period between two consecutive ground contacts of the paw of one limb. The time point of paw contact was identified visually. The stance phase lasted from the initial paw contact until liftoff, and this was followed by the swing phase, which started with liftoff and terminated with ground contact of the paw. We defined mid-stance as the time point in the middle of the stance phase. For swimming, we defined a stroke cycle as the time period between two consecutive hip angle minimums of one limb. This was determined using kinematic joint-angle measurements. Within a stroke cycle, two phases were distinguished, the 'power stroke' and the 'return stroke'. The power stroke started with the minimum hip angle and ended when the maximum hip angle was reached. The onset and ending of the return stroke was determined by the maximum and minimum hip angle, respectively. We defined the body axis, which was required for the tail kinematics, as a virtual line connecting the nose, two virtual points midway between fore- and hindlimbs and the genital area.

For evaluation of skilled walking over the horizontal ladder, steps were counted and classified as either functional paw placement (a weight-bearing step on a rung), slip (a step with initial contact of the rung followed by a slip off the rung) or miss (a step that missed the rung completely). We quantified fore-hindlimb coordination by assessing how often the same rung was targeted (touched) first by the forelimb and then by the ipsilateral hindlimb, a pattern that is usually observed in intact rodents crossing a ladder (baseline)[14]. Numbers were expressed as a percentage of total steps or targeting attempts and were an average of at least three passes.

For wading and walking, we defined the base of support as the distance between the paws during the stance phase. For the hindlimbs, base of support was calculated by adding the distances measured between the MTP of the third toe and the body axis for consecutive left-right hindlimb steps. We assessed external rotation of the hindlimb at the beginning of the stance phase by measuring the angle between the body axis and the paw axis defined by a virtual line connecting the third MTP and the heel. For evaluation of base of support and external rotation, we used the bottom view. On the basis of the side views, horizontal protraction and retraction of hind- and forelimbs in the sagittal plane were quantified by measuring the maximal and minimal toe or wrist excursions relative to the iliac crest or shoulder, respectively. The number of steps with paw dragging (defined as digits touching the ground during the swing phase) were counted and expressed as a percentage of total steps. We determined the height of the iliac crest by measuring the vertical distance between the iliac crest and the surface of the runway during mid-stance.

doi:10.1038/nmeth.1484

For swimming, the number of forelimb strokes was assessed manually. Forelimb strokes that touched the walls of the Plexiglas basin and thus were mainly used for navigation were excluded from the analysis. We evaluated left-right coordination by measuring the time interval between the onset of the stroke cycle of the ipsilateral and contralateral hindlimb. This time interval was then normalized to the duration of the complete stroke cycle of one of the hindlimbs, usually the right, and expressed as a percentage[9,35]. Thus, 0% indicates simultaneous hindlimb movements, whereas 50% suggests a perfect alternating 'out-of-phase' rhythm. Deviation from the perfect out-of-phase rhythm was used as a readout of left-right coordination. Stick diagrams, spatial displacement plots and angle-angle plots were typically generated for a time period of 1 s (four to five stroke cycles in intact rats) per pass. We evaluated tail-hindlimb coordination by determining the temporal relation between the time point of the most extreme angular displacement of the base of tail to the left or the right side and the time point of the maximal hindlimb extension.

Statistics. We performed the statistical analysis with the SPSS software package for Windows (version 14.0; SPSS) and GraphPad Prism 5 for Windows (version 5.01; GraphPad Software). For the behavioral data obtained from rats with a CNS injury, one-way repeated-measures ANOVA followed by *post hoc* Bonferroni tests were used to assess lesion effects (baseline vs. 3 or 7 d after injury) and functional recovery (3 or 7 vs. 28 d after injury). To detect correlations between parameters, we calculated Pearson's correlation coefficients. For rats with a ventral SCI, only descriptive statistics were applied because only two rats were evaluated. In these cases, results for individual rats are shown in the figures, with black and white dots representing individual rats. To test differences between *Epha4*$^{-/-}$ mice and wild-type mice, we performed Student's *t*-test (two-tailed, unpaired). Data are presented as group mean values for every testing session; error bars represent s.e.m. The level of statistical significance for all tests was set *a priori* at $P < 0.05$.

Preparation of figures. We generated the data graphs in Microsoft Office Excel 2007. Stick diagrams were generated by the ClickJoint software, version 5.0. Photographs, diagrams and all data graphs were processed in Microsoft Office PowerPoint 2007 (Microsoft) and Adobe Photoshop CS3 Extended (Adobe).

31. Schucht, P., Raineteau, O., Schwab, M.E. & Fouad, K. Anatomical correlates of locomotor recovery following dorsal and ventral lesions of the rat spinal cord. *Exp. Neurol.* **176**, 143–153 (2002).
32. Kaegi, S., Schwab, M.E., Dietz, V. & Fouad, K. Electromyographic activity associated with spontaneous functional recovery after spinal cord injury in rats. *Eur. J. Neurosci.* **16**, 249–258 (2002).
33. Fischer, M.S., Schilling, N., Schmidt, M., Haarhaus, D. & Witte, H. Basic limb kinematics of small therian mammals. *J. Exp. Biol.* **205**, 1315–1338 (2002).
34. Filipe, V.M. *et al.* Effect of skin movement on the analysis of hindlimb kinematics during treadmill locomotion in rats. *J. Neurosci. Methods* **153**, 55–61 (2006).
35. Kloos, A.D., Fisher, L.C., Detloff, M.R., Hassenzahl, D.L. & Basso, D.M. Stepwise motor and all-or-none sensory recovery is associated with nonlinear sparing after incremental spinal cord injury in rats. *Exp. Neurol.* **191**, 251–265 (2005).